# Chalmers Publication Library

# Copyright Notice

(Article begins on next page)

# On the Exact BER of Bit-Wise Demodulators for One-Dimensional Constellations

Mikhail Ivanov, Fredrik Brännström, *Member, IEEE,* Alex Alvarado, *Member, IEEE,* and Erik Agrell, *Senior Member, IEEE*

*Abstract*—The optimal bit-wise demodulator for $M$-ary pulse amplitude modulation (PAM) over the additive white Gaussian noise channel is analyzed in terms of uncoded bit-error rate (BER). The BER analysis is based on studying the bit patterns that form a labeling. New closed-form BER expressions for 4-PAM with any labeling are developed. Moreover, closed-form BER expressions for 11 out of 23 possible bit patterns for 8-PAM are presented, which enable us to obtain the BER for 8-PAM with some of the most popular labelings, including the binary reflected Gray code and the natural binary code. Numerical results show that, regardless of the labeling, there is no difference between the optimal demodulator and the symbol-wise demodulator for any BER of practical interest (below $0.1$).

*Index Terms*—Additive white Gaussian noise channel, binary reflected Gray code, bit error probability, bit-interleaved coded modulation, demapper, demodulator, LLRs, logarithmic likelihood ratio, pulse-amplitude modulation, uncoded transmission.

## I. INTRODUCTION AND MOTIVATION

Current wireless communication systems are based on the bit-interleaved coded modulation (BICM) paradigm introduced in [1] and later studied in [2], [3]. One key element in these systems is the demodulator which calculates logarithmic likelihood ratios (LLR, also known as L-values) for the received bits, which are then passed to the channel decoder. The calculation of L-values is crucial in many other coded systems. The coded performance analysis of BICM systems is generally not straightforward and is usually carried out either numerically by Monte-Carlo simulation or in terms of lower and upper bounds [2, Sec. 4], [3, Ch. 4]. In this paper, we analyze the *uncoded* performance of bit-wise demodulators over the additive white Gaussian noise (AWGN) channel.

The optimal bit-wise demodulator (BD) minimizing the BER implies the calculation of (exact) L-values for the received bits. The uncoded performance of such a demodulator has been studied in [4], where closed-form expressions for the BER for 4-PAM with the binary reflected Gray code (BRGC) [5]–[7] are presented. Due to the complexity of the BD, the calculation of L-values in practical systems is usually done based on the so-called max-log approximation [8, eq. (5)], [9, eq. (1)]. We call this demodulator the approximate BD (ABD). The ABD is equivalent to the symbol detector in terms of uncoded BER [10, Sec. IV-A], whose performance is well documented in literature, e.g., [11, Ch. 5], [12, Ch. 10], [6], [13]–[18] and references therein.

It is well known that the uncoded BER of one-dimensional constellation can be expressed as a sum of Gaussian Q-functions, cf. [11, Ch. 5], [12, Ch. 10] and references therein. The arguments of the Q-functions depend on the points that separate the decision regions associated with different bits. We refer to these points as thresholds. In [19], we generalized the BER expression to any one-dimensional constellation. The computation of the thresholds for the BD—the optimal bit-wise demodulator—is in general complicated and unknown. In this paper, however, we show that this problem can be solved analytically for 4-PAM and any labeling, extending the results presented in [4]. Moreover, we also analytically calculate the thresholds for 8-PAM with some relevant labelings, including the BRGC, the natural binary labeling (NBC) [20, Sec. II-B], the folded binary code (FBC) [16] [20, Sec. II-B], the binary semi-Gray code (BSGC) [20, Sec. II-B], and the anti-Gray code (AGC) [21]. Numerical results show that optimal and suboptimal demodulators are different in terms of the BER only at a very low SNR. At BER below $0.1$ there is no notable difference between them.

The rest of the paper is organized as follows. In Sec. II we introduce the notation convention, the system model, and the two demodulators. In Sec. III the BER analysis is presented. The patterns that form a labeling are studied in Sec. III-D. The threshold computation for the BD is shown in Sec. IV and the numerical results in Sec. V. The conclusions are drawn in Sec. VI.

## II. PRELIMINARIES

### A. Notation Convention

In this paper the following notation is used. Lowercase letters $x$ denote real or complex scalars and boldface letters $\boldsymbol{x}$ denote a row vector of scalars. The complex conjugate of $x$ is denoted by $x^*$. Blackboard bold letters $\mathbb{X}$ denote matrices with elements $x_{i,j}$ in the $i$th row and the $j$th column and $(\cdot)^\mathsf{T}$ denotes transposition. Calligraphic capital letters $\mathcal{X}$ denote sets, where the set of real numbers is denoted by $\mathcal{R}$. The binary complement of $x \in \{0, 1\}$ is denoted by $\bar{x} = 1 - x$ and its bipolar representation by $\tilde{x} = 2x - 1$.

Mikhail Ivanov, Fredrik Brännström, and Erik Agrell are with the Dept. of Signals and Systems, Chalmers Univ. of Technology, SE-41596 Gothenburg, Sweden (e-mails: {mikhail.ivanov, fredrik.brannstrom, agrell}@chalmers.se).

Alex Alvarado is with the Dept. of Engineering, Univ. of Cambridge, Cambridge CB2 1PZ, United Kingdom (e-mail: alex.alvarado@ieee.org).

Binary addition (exclusive-OR) of two bits $a$ and $b$ is denoted by $a \oplus b$. Random variables are denoted by capital letters $X$ and probabilities by $\Pr\{\cdot\}$. The Gaussian Q-function is defined as $Q(x) \triangleq (1/\sqrt{2\pi}) \int_x^\infty \exp(-t^2/2)\,dt$.

### B. System Model

In this paper we analyze a system where a vector of binary data $\boldsymbol{b} = [b_1, \ldots, b_m]$ is fed to a modulator. The modulator carries out a one-to-one mapping from $\boldsymbol{b}$ to one of the $M$ constellation points $x \in \mathcal{X} = \{s_1, \ldots, s_M\}$ for transmission over the physical channel, where $M = 2^m$. We assume that $s_1 < s_2 < \ldots < s_M$.

The modulator is determined by the constellation and its binary labeling. A binary labeling is specified by the matrix $\mathbb{C} = [\boldsymbol{c}_1^\mathsf{T}, \ldots, \boldsymbol{c}_M^\mathsf{T}]^\mathsf{T}$ of dimensions $M$ by $m$, where the $i$th row $\boldsymbol{c}_i = [c_{i,1}, \ldots, c_{i,m}]$ is the binary label of the constellation point $s_i$.

For PAM constellations, $s_i = -d(M - 2i + 1), i = 1, \ldots, M$, where $d = \sqrt{3/(M^2 - 1)}$ to normalize the constellation to unit average energy, i.e., $E_s = (1/M) \sum_{i=1}^M s_i^2 = 1$. We assume bits transmitted in the $j$th position $B_j$ to be independent and identically distributed (i.i.d.) with $\Pr\{B_j = u\} = 0.5, \forall j$ and $u \in \{0, 1\}$, and thus, the symbols are equiprobable, i.e., $\Pr\{X = s_i\} = 1/M, \forall i$.

In this paper we consider a discrete time memoryless AWGN channel with output $y = x + \eta$, where $x \in \mathcal{X}$ and the noise sample $\eta$ is a zero-mean Gaussian random variable with variance $N_0/2$. The conditional probability density function (PDF) of the channel output given channel input is

$$p_{Y|X}(y|x) = \sqrt{\frac{\gamma}{\pi}} e^{-\gamma(y-x)^2}, \tag{1}$$

where the average signal to noise ratio (SNR) is defined as $\gamma \triangleq E_s/N_0 = 1/N_0$.

The observation $y$ is used by the demodulator to decide on the received binary sequence, i.e., to produce $\hat{\boldsymbol{b}} = [\hat{b}_1, \ldots, \hat{b}_m]$. In this paper we consider two demodulators to obtain $\hat{\boldsymbol{b}}$ from $y$, which are described in the next section.

### C. Demodulators

The BD calculates (a posteriori) L-values for the $m$ bits based on the observation $y$, i.e.,

$$l_j(y) \triangleq \log \frac{\Pr\{B_j = 1|Y = y\}}{\Pr\{B_j = 0|Y = y\}} \tag{2}$$

$$= \log \frac{\sum_{x \in \mathcal{X}_{j,1}} e^{-\gamma(y-x)^2}}{\sum_{x \in \mathcal{X}_{j,0}} e^{-\gamma(y-x)^2}}, \tag{3}$$

for $j = 1, \ldots, m$ and $\mathcal{X}_{j,u} \triangleq \{s_i \in \mathcal{X} : c_{i,j} = u, \forall i\}$. To pass from (2) to (3) Bayes' rule was used together with the i.i.d. assumption of the bits and the conditional PDF in (1). The BD uses the L-values in (3) to make a decision on the received bit according to the rule

$$\hat{b}_j^{\mathrm{BD}} = \begin{cases} 1 & \text{if } l_j(y) \geq 0, \\ 0 & \text{otherwise.} \end{cases} \tag{4}$$

The implementation of the BD in its exact form (3) is complicated, especially for large constellations, as it requires calculation of the logarithm of a sum of exponentials. To overcome this problem, approximations are usually used in practice. The most common approximation is the so-called max-log approximation ($\log \sum_i e^{\lambda_i} \approx \max_i \lambda_i$) [1, eq. (3.2)], [2, eq. (9)], [8, eq. (5)], [22, eq. (8)], which used in (3) gives

$$\tilde{l}_j(y) = \gamma \left[ \min_{x \in \mathcal{X}_{j,0}} (y - x)^2 - \min_{x \in \mathcal{X}_{j,1}} (y - x)^2 \right]. \tag{5}$$

The use of the max-log approximation transforms the nonlinear relationship (3) into a piece-wise linear relationship (5), as previously shown in e.g., [23, Fig. 3], [24, eqs. (11)–(14)]. Simplifications of (5) were studied in [25] and [26].

The ABD is defined as the demodulator that applies the same decision rule (4) based on L-values calculated by (5). As mentioned in [10, Sec. IV-A] and proved in [19, Theorem 1] the ABD is equivalent to the symbol detector in terms of uncoded BER.

## III. BER for One-Dimensional Constellations

The BER for a given labeling $\mathbb{C}$ can be expressed as

$$P_{\mathbb{C}} = \frac{1}{m} \sum_{j=1}^m P_j, \tag{6}$$

where using the law of total probability, the BER for the $j$th bit position $P_j \triangleq \Pr\{\hat{B}_j \neq b_j | B_j = b_j\}$ can be written as

$$P_j = \frac{1}{M} \sum_{i=1}^M \Pr\{\hat{B}_j \neq c_{i,j} | X = s_i\}. \tag{7}$$

The BER for the $j$th bit position $P_j$ depends only on the subconstellations $\mathcal{X}_{j,0}$ and $\mathcal{X}_{j,1}$ (cf. (3)–(5)), i.e., $P_j$ is a function of the $j$th column of $\mathbb{C}$. The matrix $\mathbb{C}$ consists of $m$ columns, one column for each bit position. We refer to these columns as patterns which are formally defined below.

We define a bit pattern (or simply pattern) as a length-$M$ binary vector $\boldsymbol{p} = [p_1, \ldots, p_M] \in \{0, 1\}^M$ with Hamming weight $M/2$. The labeling $\mathbb{C}$ can now be defined by $m$ patterns, each corresponding to one column of $\mathbb{C}$. We index the patterns as $\boldsymbol{p}_w$ with $w$ being the decimal representation of the vector $\boldsymbol{p}$, i.e., $w = \sum_{i=1}^M 2^{M-i} p_i$. For example, for $M = 4$, the pattern $[0, 1, 0, 1]$ is indexed as $\boldsymbol{p}_5$. The BER for the labeling $\mathbb{C}$ does not depend on the order of its columns, and thus, the BER for the labeling $\mathbb{C}$ is fully determined by a set of $m$ patterns (indices) $\mathcal{W} = \{w_1, \ldots, w_m\}$. Examples of common labelings and the patterns they consist of for 4-PAM and 8-PAM are given in Table II. Based on the previous discussion, from now on we concentrate our analysis only on patterns (and not on labelings).

To analyze the BER of a pattern (PBER), the observation space $\mathcal{R}$ is split into two disjoint decision regions, i.e., $\mathcal{Y}_0 = \{y \in \mathcal{R} : \hat{b} = 0\}$ and $\mathcal{Y}_1 = \{y \in \mathcal{R} : \hat{b} = 1\}$ such that $\mathcal{Y}_0 \cup \mathcal{Y}_1 = \mathcal{R}$. Using the definition of $\mathcal{Y}_0$ and $\mathcal{Y}_1$, the PBER for the pattern $\boldsymbol{p} = [p_1, \ldots, p_M]$ can be rewritten as

$$P = \frac{1}{M} \sum_{i=1}^M \Pr\{Y \in \mathcal{Y}_{\bar{p}_i} | X = s_i\}. \tag{8}$$
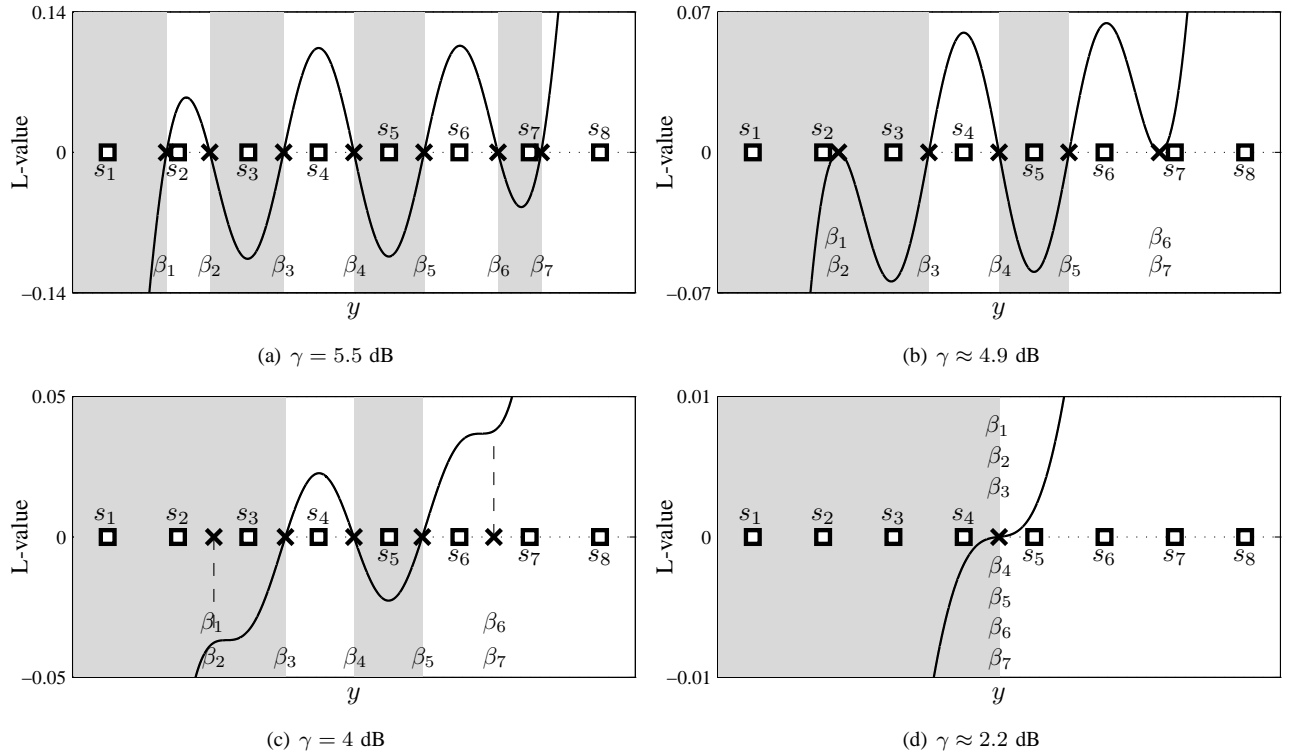
Fig. 1. L-values in (3) vs. the received signal for different $\gamma$ for 8-PAM and the BD for $\boldsymbol{p}_{85} = [0, 1, 0, 1, 0, 1, 0, 1]$. Squares show the constellation points and crosses show the thresholds $\beta_k$ in Theorem 5. Gray and white areas indicate $\mathcal{Y}_0$ and $\mathcal{Y}_1$, resp. In (a) at $\gamma = 5.5$ dB none of the seven thresholds is virtual. At $\gamma \approx 4.9$ dB, shown in (b), the thresholds $\beta_1$ and $\beta_2$ as well as $\beta_6$ and $\beta_7$ become virtual, shown also in (c) for $\rho = 4$ dB. At $\gamma \approx 2.2$ dB, shown in (d), $\beta_3$ and $\beta_5$ merge with $\beta_4$ and also become virtual.

By expressing $P$ as in (8), it is clear that the PBER in (7) can be calculated using the decision region $\mathcal{Y}_0$ only, as opposed to alternative approaches where (8) is expressed in terms of the PDF of the L-values [27, eq. (19)].

*A. Decision Thresholds*

One key element in the BER analysis presented in this paper is the *decision thresholds*. Decision thresholds (or simply thresholds) for a given pattern $\boldsymbol{p}$ are the points that separate the decision regions for zeros and ones, and thus, they determine the PBER for the BD/ABD in (8). For a given pattern $\boldsymbol{p}$, we associate the threshold $\beta_k \in \mathcal{R}$ to the bit $p_k$ when $p_k \neq p_{k+1}$. Since there is no threshold $\beta_k$ when $p_k = p_{k+1}$, the number of thresholds is at most $M - 1$. The indices of the thresholds for the pattern $\boldsymbol{p}$ form a set of indices $\mathcal{K}$, with $1 \leq |\mathcal{K}| \leq M - 1$. For example, the pattern $\boldsymbol{p}_{54} = [0, 0, 1, 1, 0, 1, 1, 0]$ has $\mathcal{K} = \{2, 4, 5, 7\}$. $\mathcal{K}$ contains four elements indicating that there are four thresholds associated with the second, the fourth, the fifth, and the seventh bits in the pattern $\boldsymbol{p}_{54}$.

The thresholds for the ABD, which we denote by $\tilde{\beta}$, are independent of $\gamma$ and placed at the midpoints between adjacent constellation points with different binary labels, which follows directly from (5). On the other hand, the thresholds for the BD depend on $\gamma$. We denote these thresholds by $\beta$, where to simplify the notation, the dependency on $\gamma$ is omitted. From (3) it is clear that the L-value is a function of the observation. For a given SNR the problem of finding the thresholds can be solved graphically by finding the points

where the function $l_j(y)$ crosses the zero-level. Fig. 1 shows the BD thresholds for $\boldsymbol{p}_{85} = [0, 1, 0, 1, 0, 1, 0, 1]$ for four different SNR values. This figure shows that some thresholds can merge at low SNR and seem to disappear. To take this effect into account, we define virtual thresholds as follows. A threshold $\beta_k$ is said to be *virtual* at $\gamma < \gamma_0$ if it merges with another threshold $\beta_{k'}$ at $\gamma = \gamma_0$ (i.e., $\beta_k = \beta_{k'}$ when $\gamma = \gamma_0$) and does not exist at $\gamma < \gamma_0$.

*B. General Expression for One-Dimensional Constellations*

The BER expression for the ABD and an $M$-PAM constellation with any labeling is well known and can be found in [7, eq. (21)]. The PBER expression can easily be obtained in a similar way. In [19, Theorem 2] the PBER expression for the ABD was generalized to any one-dimensional constellation. In the following theorems we generalize this expression to the BD, first, assuming that none of the thresholds $\beta_k$ is virtual, and second, extending the results to the virtual threshold case.

*Theorem 1:* The PBER of the BD or the ABD using an arbitrary one-dimensional constellation with a pattern $\boldsymbol{p}$ can be expressed as

$$P = \frac{1}{2} + \frac{1}{M} \sum_{i=1}^{M} \sum_{k \in \mathcal{K}} g_{i,k} Q\left((\beta_k - s_i)\sqrt{2\gamma}\right), \quad (9)$$

where none of the $\beta_k$ is virtual, and $g_{i,k} \in \{\pm 1\}$ is

$$g_{i,k} \triangleq (p_{k+1} - p_k)(1 - 2p_i). \quad (10)$$

*Proof:* We define a set $\bar{\mathcal{K}} = \{1, \ldots, M-1\} \setminus \mathcal{K}$. For each $k' \in \bar{\mathcal{K}}$ we define a value $\beta_{k'}$ equal to the nearest threshold $\beta_k$, i.e., $\beta_{k'} = \beta_k$ where $k' \in \bar{\mathcal{K}}$ and $k = \arg\min_{j \in \mathcal{K}} |j - k'|$. Using the values $\beta_k$, $k = 1, \ldots, M-1$ as thresholds, the proof follows directly from [19, eq. (11)] using the fact that $g_{i,k} = 0$ for $k \in \bar{\mathcal{K}}$ and any $i$. $\square$

The following theorem shows that Theorem 1 also holds when some of the thresholds become virtual, provided that their values are chosen properly.

*Theorem 2:* When a threshold $\beta_k$ merges with another threshold $\beta_{k'}$ at SNR $\gamma_0$ (i.e, $\beta_k$ becomes virtual), the PBER for the BD can be calculated for any SNRs below $\gamma_0$ using (9)–(10) with $\beta_k = \beta_{k'}$.

*Proof:* We will show that the PBER in (9) is not affected by the virtual threshold $\beta_k$ if $\beta_k = \beta_{k'}$. Without loss of generality assume $k' > k$. Let $S_i$ be the two terms in the inner sum in (9) associated with the thresholds $\beta_k$ and $\beta_{k'}$, i.e.,

$$S_i \triangleq g_{i,k} Q\Big((\beta_k - s_i)\sqrt{2\gamma}\Big) + g_{i,k'} Q\Big((\beta_{k'} - s_i)\sqrt{2\gamma}\Big). \quad (11)$$

Since $\beta_k$ and $\beta_{k'}$ are thresholds that merge, $p_{k+1} = p_{k'}$ and $p_k = p_{k'+1}$ must hold. Using these relations in (10), we obtain $g_{i,k} = -g_{i,k'}$, which used in (11) gives $S_i = 0$, $\forall i$ if $\beta_k = \beta_{k'}$. $\square$

*Remark 1:* Theorem 2 holds regardless of whether $\beta_{k'}$ is virtual or not. If $\beta_{k'}$ is not virtual for $\gamma < \gamma_0$, $\beta_k$ must be set to the value of $\beta_{k'}$ for $\gamma < \gamma_0$. If $\beta_{k'}$ is virtual for $\gamma < \gamma_0$, $\beta_k = \beta_{k'}$ can be set to any real value.

### C. BER for the ABD and $M$-PAM

For $M$-PAM and the ABD, the PBER can be expressed as a bit-wise version of [7, eq. (21)] by using mid-points as thresholds and combining Q-functions with the same arguments in (9)

$$\tilde{P} = \frac{1}{M} \sum_{n=1}^{M-1} a_n Q\Big((2n-1)d\sqrt{2\gamma}\Big), \quad (12)$$

where

$$a_n = \sum_{k=n}^{M-1} (p_{k+1} - p_k)(1 - 2p_{k+1-n})$$
$$- (p_{k+2-n} - p_{k+1-n})(1 - 2p_{k+1}). \quad (13)$$

The values $a_n$ correspond to values in [7, eq. (22)] calculated for a pattern instead of a labeling and scaled by a factor $2M$. The element $a_1$ is equal to twice the number of pairs of constellation points at minimum ED whose bits are different (for a given pattern). For example, $a_1 = 2$ for patterns of the form $p = [0, \ldots, 0, 1, 1, \ldots 1]$ as there is only one pair of points at minimum ED.

One direct consequence of (12) is that the vector $\boldsymbol{a} \triangleq [a_1, \ldots, a_{M-1}]$ with $a_n$ given by (13) completely defines the performance of the ABD for $M$-PAM and allows us to compare the performance of different patterns. From (12), the PBER for high SNR is determined by the coefficient

TABLE I
CLASSES OF PATTERNS FOR 4-PAM WITH THEIR CORRESPONDING REPRESENTATIVES $\boldsymbol{p}$, TYPES, DECIMAL REPRESENTATIONS OF THE PATTERNS $w$, VECTORS $\boldsymbol{a}$ DEFINING THE PBER FOR THE ABD, AND THRESHOLDS FOR THE REPRESENTATIVES

| $q$ | $\boldsymbol{p}$ | Type | $w$ | $\boldsymbol{a}$ | Thresholds |
|---|---|---|---|---|---|
| 1 | $[0, 0, 1, 1]$ | ARE | **3** 12 | $[2, \quad 2, \quad 0]$ | $\beta_2 = 0$ |
| 2 | $[0, 1, 1, 0]$ | RE | **6** 9 | $[4, \quad 2, -2]$ | $\beta_3 = -\beta_1$ |
| 3 | $[0, 1, 0, 1]$ | ARE | **5** 10 | $[6, -4, \quad 2]$ | $\beta_3 = -\beta_1, \beta_2 = 0$ |

multiplying the Q-function with the smallest argument, i.e., $a_1$. If two patterns have identical coefficients $a_1$, the next coefficients $a_2$ should be compared, and so on.

Using (6) and (12), the average BER for an $M$-PAM with a labeling $\mathbb{C}$ can be expressed as

$$\tilde{P}_{\mathbb{C}} = \frac{1}{mM} \sum_{n=1}^{M-1} \alpha_n Q\Big((2n-1)d\sqrt{2\gamma}\Big), \quad (14)$$

where $\boldsymbol{\alpha} \triangleq [\alpha_1, \ldots, \alpha_{M-1}]$ is the sum of vectors $\boldsymbol{a}$ for the $m$ patterns used in $\mathbb{C}$. The equation in (14) in fact corresponds to [7, eq. (21)], where the value of $\alpha_n$ is a scaled version of the so-called differential average distance spectrum $\bar{\delta}(n, \lambda)$, i.e., $\alpha_n = 2M\bar{\delta}(n, \lambda)$.

### D. Bit Patterns

We distinguish between three types of patterns [19]. The pattern $\boldsymbol{p}$ is said to be *reflective* (RE) if $p_i = p_{M+1-i}$ for $i = 1, \ldots, M$. The pattern $\boldsymbol{p}$ is said to be *anti-reflective* (ARE) if $p'_i = \bar{p}_i$ for $i = 1, \ldots, M$. Finally, the pattern $\boldsymbol{p}$ is called *asymmetric* (ASY) if it is neither RE nor ARE. For example, $\boldsymbol{p}_{60} = [0, 0, 1, 1, 1, 1, 0, 0]$ is an RE pattern, $\boldsymbol{p}_{43} = [0, 0, 1, 0, 1, 0, 1, 1]$ is an ARE pattern, and $\boldsymbol{p}_{216} = [1, 1, 0, 1, 1, 0, 0, 0]$ is an ASY pattern.

As it was shown in [19, Sec. IV], for $M$-PAM all the length-$M$ bit patterns can be grouped into $Q$ classes, where

$$Q = \frac{1}{4}\left(\binom{M}{M/2} + \binom{M/2}{M/4} + 2^{M/2}\right). \quad (15)$$

All the patterns within one class have the same PBER and each class is represented by a unique class index $q \in \{1, \ldots, Q\}$, shown in the first column of Tables I and III. All the patterns within one class have the same PBER. For 4-PAM there are six patterns which are grouped into $Q = 3$ classes as shown in Table I. As an example, one of the patterns of a class is shown in the second column. These patterns are called *representative* and are used to analyze the PBER of the patterns in the class. Three labelings that give different BER for 4-PAM are listed in the first part of Table II.

For 8-PAM ($M = 8$), there are $Q = 23$ classes of patterns, 11 of them are either reflective or anti-reflective and they are shown in the first 11 rows of Table III and ordered from the best to worst PBER for high SNR, as predicted by the vectors $\boldsymbol{a}$. The 12 classes of asymmetric patterns are listed in the last 12 rows of Table III and also ordered in a similar way. As shown in [19], there are 460 labelings that give different BER and five of the most common ones are shown in the second part of Table II (listed from best to worst).

TABLE III
CLASSES OF PATTERNS FOR 8-PAM WITH THEIR CORRESPONDING REPRESENTATIVES $p$, TYPES, DECIMAL REPRESENTATIONS OF THE PATTERNS $w$, VECTORS $a$ DEFINING THE PBER FOR THE ABD, AND THRESHOLDS FOR THE REPRESENTATIVES

| $q$ | $p$ | Type | $w$ | $a$ | Thresholds |
|---|---|---|---|---|---|
| 1 | $[0,0,0,0,1,1,1,1]$ | ARE | **15** 240 | $[\;2,\;\;2,\;\;2,\;\;2,\;\;0,\;\;0,\;\;0]$ | $\beta_4 = 0$ |
| 2 | $[0,0,1,1,1,1,0,0]$ | RE | **60** 195 | $[\;4,\;\;4,\;\;2,\;\;2,-2,-2,\;\;0]$ | $\beta_6 = -\beta_2 = f(t_2)$ |
| 3 | $[1,1,1,0,1,0,0,0]$ | ARE | 23 **232** | $[\;6,-2,\;\;2,\;\;0,\;\;2,\;\;0,\;\;0]$ | $\beta_5 = -\beta_3 = f(t_1),\ \beta_4 = 0$ |
| 4 | $[0,1,1,1,0,0,0,1]$ | ARE | **113** 142 | $[\;6,\;\;4,\;\;4,-4,-2,-2,\;\;2]$ | $\beta_7 = -\beta_1 = f(t_2),\ \beta_4 = 0$ |
| 5 | $[0,0,1,1,0,0,1,1]$ | ARE | **51** 204 | $[\;6,\;\;6,-4,-4,\;\;2,\;\;2,\;\;0]$ | $\beta_6 = -\beta_2 = f(t_2),\ \beta_4 = 0$ |
| 6 | $[0,1,1,0,0,1,1,0]$ | RE | **102** 153 | $[\;8,\;\;6,-6,-4,\;\;4,\;\;2,-2]$ | $\beta_7 = -\beta_1 = f(t_2),\ \beta_5 = -\beta_3 = f(t_3)$ |
| 7 | $[0,0,1,0,1,0,1,1]$ | ARE | **43** 212 | $[10,-6,\;\;4,-2,\;\;0,\;\;2,\;\;0]$ | $\beta_6 = -\beta_2 = f(t_2),$ $\beta_5 = -\beta_3 = f(t_3),\ \beta_4 = 0$ |
| 8 | $[0,1,0,0,1,1,0,1]$ | ARE | **77** 178 | $[10,\;\;0,-6,\;\;2,\;\;4,-4,\;\;2]$ | $\beta_7 = -\beta_1 = f(t_2),$ $\beta_6 = -\beta_2 = f(t_3),\ \beta_4 = 0$ |
| 9 | $[0,1,1,0,1,0,0,1]$ | ARE | **105** 150 | $[10,\;\;0,-4,\;\;6,-4,-2,\;\;2]$ | $\beta_7 = -\beta_1 = f(t_2),$ $\beta_5 = -\beta_3 = f(t_3),\ \beta_4 = 0$ |
| 10 | $[1,0,1,0,0,1,0,1]$ | RE | 90 **165** | $[12,-6,\;\;0,\;\;6,-6,\;\;4,-2]$ | $\beta_7 = -\beta_1 = f(t_1),$ $\beta_6 = -\beta_2 = f(t_3),\ \beta_5 = -\beta_3 = f(t_2)$ |
| 11 | $[0,1,0,1,0,1,0,1]$ | ARE | **85** 170 | $[14,-12,10,-8,6,-4,2]$ | $\beta_7 = -\beta_1 = f(t_2),\ \beta_6 = -\beta_2 = f(t_3),$ $\beta_5 = -\beta_3 = f(t_1),\ \beta_4 = 0$ |
| 12 | $[0,0,0,1,1,1,1,0]$ | ASY | **30** 120 135 225 | $[\;4,\;\;3,\;\;3,\;\;2,-2,-1,-1]$ | $\beta_3, \beta_7$ |
| 13 | $[0,0,0,1,1,1,0,1]$ | ASY | **29** 71 184 226 | $[\;6,\;\;1,\;\;2,-3,\;\;1,\;\;0,\;\;1]$ | $\beta_3, \beta_6, \beta_7$ |
| 14 | $[0,0,0,1,1,0,1,1]$ | ASY | **27** 39 216 228 | $[\;6,\;\;2,-3,\;\;1,\;\;1,\;\;1,\;\;0]$ | $\beta_3, \beta_5, \beta_6$ |
| 15 | $[0,0,1,1,1,0,0,1]$ | ASY | **57** 99 156 198 | $[\;6,\;\;5,\;\;0,-3,-3,\;\;2,\;\;1]$ | $\beta_2, \beta_5, \beta_7$ |
| 16 | $[0,0,1,0,1,1,1,0]$ | ASY | **46** 116 139 209 | $[\;8,-1,2,-1,3,-2,-1]$ | $\beta_2, \beta_3, \beta_4, \beta_7$ |
| 17 | $[0,0,1,1,1,0,1,0]$ | ASY | **58** 92 163 197 | $[\;8,-1,3,-2,2,-1,-1]$ | $\beta_2, \beta_5, \beta_6, \beta_7$ |
| 18 | $[0,1,0,0,1,1,1,0]$ | ASY | **78** 114 141 177 | $[\;8,\;2,-1,-1,-1,3,-2]$ | $\beta_1, \beta_2, \beta_4, \beta_7$ |
| 19 | $[0,0,1,1,0,1,1,0]$ | ASY | **54** 108 147 201 | $[\;8,\;3,-6,3,3,-2,-1]$ | $\beta_2, \beta_4, \beta_5, \beta_7$ |
| 20 | $[0,0,1,0,1,1,0,1]$ | ASY | **45** 75 180 210 | $[10,-3,-3,6,-4,1,1]$ | $\beta_2, \beta_3, \beta_4, \beta_6, \beta_7$ |
| 21 | $[0,0,1,1,0,1,0,1]$ | ASY | **53** 83 172 202 | $[10,-3,1,0,-2,1,1]$ | $\beta_2, \beta_4, \beta_5, \beta_6, \beta_7$ |
| 22 | $[0,1,0,1,1,0,0,1]$ | ASY | **89** 101 154 166 | $[10,\;0,-3,1,1,-3,2]$ | $\beta_1, \beta_2, \beta_3, \beta_5, \beta_7$ |
| 23 | $[0,1,0,1,0,1,1,0]$ | ASY | **86** 106 149 169 | $[12,-6,3,-1,-1,3,-2]$ | $\beta_1, \beta_2, \beta_3, \beta_4, \beta_5, \beta_7$ |

TABLE II
SOME COMMON LABELINGS FOR 4-PAM AND 8-PAM WITH THEIR CORRESPONDING PATTERNS INDICES $\mathcal{W}$, AND VECTORS $\alpha$ DEFINING THE BER FOR THE ABD

| $M$ | Labeling | $\mathcal{W}$ | $\alpha$ |
|---|---|---|---|
| 4 | BRGC | $\{3, 6\}$ | $[6, 4, -2]$ |
| 4 | NBC | $\{3, 5\}$ | $[8, -2, 2]$ |
| 4 | AGC | $\{5, 6\}$ | $[10, -2, 0]$ |
| 8 | BRGC | $\{15, 60, 102\}$ | $[14, 12, -2, 0, 2, 0, -2]$ |
| 8 | FBC | $\{15, 60, 90\}$ | $[18, 0, 4, 10, -8, 2, -2]$ |
| 8 | NBC | $\{15, 51, 85\}$ | $[22, -4, 8, -10, 8, -2, 2]$ |
| 8 | BSGC | $\{105, 60, 102\}$ | $[22, 10, -8, 4, -2, -2, 0]$ |
| 8 | AGC | $\{90, 105, 85\}$ | $[36, -18, 6, 4, -4, -2, 2]$ |

## IV. THRESHOLDS FOR THE BD

In this section, we show that the thresholds for the BD can be found by solving an $(M-1)$th power polynomial equation and give a closed-form solutions for 4-PAM and 8-PAM with RE and ARE patterns.

### A. Threshold Computation

The problem of finding the thresholds $\beta_k$ for the BD is equivalent to finding the solutions of $l(y) = 0$. In the following theorem we show how this can be done for $M$-PAM constellations.

*Theorem 3:* The thresholds for the BD and $M$-PAM constellations with a pattern $p$ are

$$\beta_k = \frac{1}{4\gamma d} \log z_n, \qquad (16)$$

where $z_n$ are the real and positive solutions of

$$\sum_{i=1}^{M} \check{p}_i A^{\frac{(M/2-i)(M/2+1-i)}{2}} z^{i-1} = 0, \qquad (17)$$

and

$$A = e^{-8\gamma d^2}. \qquad (18)$$

*Proof:* Using (3), $l(y) = 0$ is equivalent to $e^{l(y)} = 1$, which can be restated as finding roots of

$$h(y) \triangleq \sum_{i=1}^{M} \check{p}_i e^{-\gamma(y + d(M - 2i + 1))^2}, \qquad (19)$$
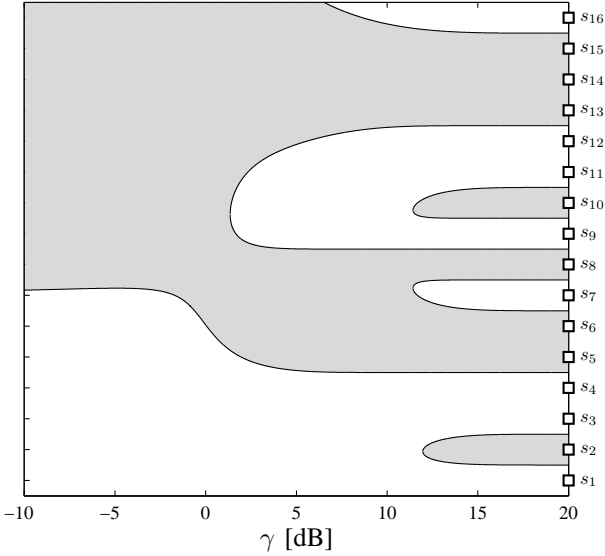
Fig. 2. Thresholds $\beta_k$ in (16) for 16-PAM with the ASY pattern $\boldsymbol{p}_{45745} = [1, 0, 1, 1, 0, 0, 1, 0, 1, 0, 1, 1, 0, 0, 0, 1]$ obtained by solving (17) numerically. The constellation points are shown with squares. Gray and white areas indicate $\mathcal{Y}_0$ and $\mathcal{Y}_1$, resp.

where the definition of the $M$-PAM symbols was used. Factorizing (19) gives

$$h(y) = e^{-\gamma y^2 - 2\gamma dy(M-1) - \gamma d^2}$$
$$\cdot \sum_{i=1}^{M} \check{p}_i e^{4\gamma dy(i-1)} e^{-8\gamma d^2 \frac{(M/2-i)(M/2+1-i)}{2}}. \quad (20)$$

Using (18) in (20) together with substitution $z = e^{4\gamma dy}$, (17) is obtained by setting $h(y) = 0$ and removing the nonzero factor preceding the summation in (20). The expression in (17) is a polynomial[1] of degree $M - 1$, and thus, it always has $M - 1$ roots. Because of the substitution $z = e^{4\gamma dy}$, only the positive (and real) roots need to be considered.

$\square$

Theorem 3 gives a general expression for finding the thresholds for $M$-PAM with any pattern $\boldsymbol{p}$. After finding the roots of (17), the thresholds $\beta_k$ may easily be obtained from (16). The main problem is that finding the roots of (17) in closed-form is, in general, not always possible. However, the roots can always be found numerically. Fig. 2 illustrates the thresholds for 16-PAM with the pattern $\boldsymbol{p}_{45745} = [1, 0, 1, 1, 0, 0, 1, 0, 1, 0, 1, 1, 0, 0, 0, 1]$ obtained by solving (17) numerically. In the following two sections we show how this problem can be solved analytically for 4-PAM and 8-PAM with RE or ARE patterns.

### B. Thresholds for 4-PAM

The following theorem shows how the thresholds are found for 4-PAM with any pattern.

---

[1]Interestingly, since $M$ is even, for $i = 1, \ldots, M$ with $i \neq M/2$ and $i \neq M/2+1$, the powers of $A$ in (17) are the so-called "triangular numbers".

*Theorem 4:* The thresholds $\beta_k$ for any pattern for 4-PAM, as listed in the last column in Table I, can be expressed as

$$\beta_1 = -\beta_3, \quad (21)$$
$$\beta_2 = 0, \quad (22)$$
$$\beta_3 = \frac{1}{4\gamma d} \log \left| \frac{1 + \check{p}_1\check{p}_4 A + \sqrt{(1+\check{p}_1\check{p}_4 A)^2 - 4A^2}}{2A} \right|, \quad (23)$$

where $A$ is given by (18).

*Proof:* The proof is given in Appendix A. $\square$

Theorem 4 gives closed-form expressions for any pattern for 4-PAM, and thus, it allows us to compute the BER for all the labelings in the first part of Table II. The results in Theorem 4 can be shown to coincide to those in [4, eq. (10)] when the BRGC is considered.

### C. Thresholds for 8-PAM

For 8-PAM, finding the thresholds for the BD requires solving a 7-power polynomial equation given by (17). This problem in general does not have a closed-form solution. However, as the following theorem shows, (17) can be reduced to a cubic equation for RE or ARE patterns. These patterns are of great value because all the most commonly studied labelings (e.g., BRGC, NBC, FBC, BSGC, AGC) can be composed from them (cf. Table II). The proposed technique, however, does not work for ASY patterns and thresholds for ASY patterns can be obtained, for instance, numerically.

*Theorem 5:* The thresholds $\beta_k$ for the patterns in the classes $q = 1, 2, \ldots, 11$ for 8-PAM can be expressed as

$$\beta_k = -\beta_{8-k} = \begin{cases} f(t_n) & \text{if } k = 5, 6, 7, \\ 0 & \text{if } k = 4, \end{cases} \quad (24)$$

$$f(t) \triangleq \frac{1}{4\gamma d} \log \left| \frac{|t| + \sqrt{|t|^2 - 4}}{2} \right|, \quad (25)$$

with

$$t_1 \triangleq \frac{1}{6\check{p}_1 A^3} \left( T + \frac{2\sqrt[3]{2}C}{B} + \sqrt[3]{4}B \right), \quad (26)$$

$$t_2 \triangleq \frac{1}{6\check{p}_1 A^3} \left( T - \frac{\sqrt[3]{2}(1+\sqrt{3}\jmath)C}{B} - \frac{1-\sqrt{3}\jmath}{\sqrt[3]{2}}B \right), \quad (27)$$

$$t_3 \triangleq \frac{1}{6\check{p}_1 A^3} \left( T - \frac{\sqrt[3]{2}(1-\sqrt{3}\jmath)C}{B} - \frac{1+\sqrt{3}\jmath}{\sqrt[3]{2}}B \right), \quad (28)$$

$A$ is given by (18),

$$T \triangleq 2(\check{p}_8 A^3 - \check{p}_2), \quad (29)$$

$$B \triangleq \sqrt[3]{\sqrt{D^2 - 4C^3} - \check{p}_1\check{p}_8 D}, \quad (30)$$

$$C \triangleq 7A^6 + \check{p}_2\check{p}_8 A^3 - 3\check{p}_1\check{p}_3 A + 1, \quad (31)$$

$$D \triangleq 7\check{p}_1 A^9 - 12\check{p}_1\check{p}_2\check{p}_8 A^6 - 18\check{p}_3 A^4$$
$$+ 3\check{p}_1(1 + 9\check{p}_4\check{p}_8)A^3 - 9\check{p}_2\check{p}_3\check{p}_8 A + 2\check{p}_1\check{p}_2\check{p}_8, \quad (32)$$

and the relationship between $k$ and $n$ in (24) for the different classes $q$ is listed in the last column of Table III. As the relationship between $n$ and $k$ depends on the particular pattern, the representative of the class (the second column of Table III) should be used in the presented equations.
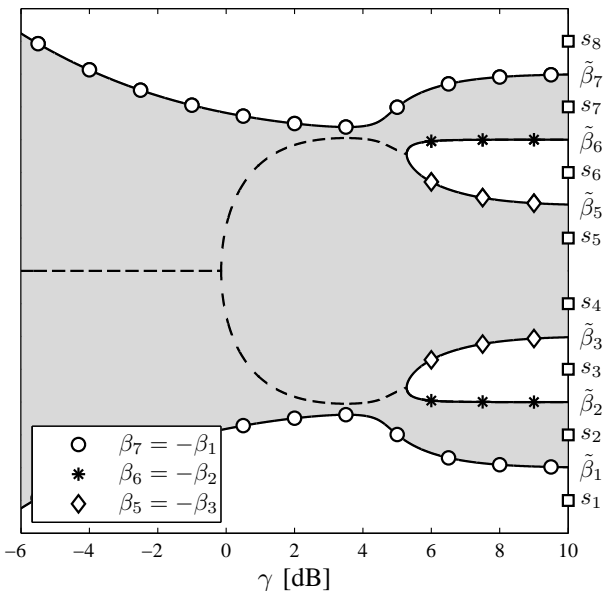
Fig. 3. The thresholds for $\boldsymbol{p}_{165} = [1, 0, 1, 0, 0, 1, 0, 1]$ ($q = 10$) for 8-PAM in Theorem 5 vs. SNR. Virtual thresholds are shown with dashed lines. The thresholds for the ABD $\tilde{\beta}_k$ and the constellation points (squares) are also shown. Gray and white areas indicate $\mathcal{Y}_0$ and $\mathcal{Y}_1$, resp.



Fig. 4. The PBER for 8-PAM with ARE ($q = 3$) and RE ($q = 10$) patterns and ASY patterns ($q = 16, 22$). Solid lines correspond to the BD and dashed lines to the ABD. The threshold for the BD were obtained using Theorem 5 for $q = 3, 10$ (the thresholds for $q = 10$ are shown in Fig. 3) and solving (17) numerically for $q = 16, 22$.

*Proof:* The proof is given in Appendix B. □

Theorem 5 shows how to analytically obtain the thresholds for the BD with 8-PAM and any RE or ARE pattern, for instance, thresholds shown in Fig. 1. Using these results, the PBER can be calculated using (9), which gives PBER expressions for 11 out of 23 classes, or equivalently, for 56 different labelings, including the 5 shown in the second part of Table II.

*Remark 2:* In the high SNR regime, i.e., $\gamma \to \infty$, all the thresholds in Theorems 4 and 5 tend to midpoints, i.e., the same constant thresholds used in the ABD for all SNR. This fact can easily be proven analytically for 4-PAM by evaluating $\lim_{\gamma \to \infty} \beta_3$ and applying l'Hôpital's rule. For 8-PAM a similar proof exists, however, in this case it is not straightforward due to the complexity of the threshold expressions. These results can be intuitively understood from the fact that the max-log approximation in (5) becomes more precise when the SNR increases, and hence, the thresholds for the BD and ABD are expected to coincide when $\gamma \to \infty$.

## V. Numerical Results

In Fig. 3 we show the thresholds given by Theorem 5 for the pattern $\boldsymbol{p}_{165}$ ($q = 10$) for 8-PAM. The figure is symmetric with respect to zero due to the symmetry of the pattern. At $\gamma \approx 5.3$ dB the pairs of thresholds $\beta_2$ and $\beta_3$, and $\beta_5$ and $\beta_6$ merge and become virtual for all $\gamma < 5.3$ dB. All the virtual thresholds shown with dashed lines satisfy the conditions in Theorem 2. As expected (see Remark 2), when $\gamma \to \infty$, the BD thresholds coincide with the ABD thresholds.

The PBER for 8-PAM with some selected patterns from Table III using (9) is presented in Fig. 4. The thresholds are calculated analytically for $q = 3, 10$ and numerically for

$q = 16, 22$. For very low SNR the gap between the BD and the ABD can reach up to several dB, however, this gap decreases when the SNR increases. The same conclusion can be drawn for all other patterns except for $q = 1$, as in this case only one threshold exists $\beta_{M/2} = 0$ for all SNR. Hence, for $q = 1$ the BD and the ABD have the same performance for $M$-PAM. To conclude, we present in Fig. 5 the BER for 8-PAM with the labelings in Table II. From the presented results we conclude that the BD outperforms the ABD, however, for any BER of practical interest (below 0.1), the difference between the BD and the ABD is negligible.

## VI. Conclusions

We proposed a general approach for estimating the performance of the optimal bit-wise demodulator and presented closed-form expressions for the BER for 4-PAM and 8-PAM with different labelings. We conclude that a suboptimal symbol-wise demodulator shows no loss compared to the optimal demodulator for all the SNR of interest, which justifies its use in practical systems.

All results presented in this paper can be easily generalized to any $N$-dimensional constellation obtained as a direct product of $N$ PAM constellations, with the labeling obtained as a direct product of the corresponding PAM labelings. This generalization includes 16-QAM and 64-QAM labeled with the BRGC.

The proposed technique for finding the zero crossings of the L-values for 8-PAM works only for reflective or anti-reflective patterns, which includes 11 out of 23 classes of patterns. Extending these results to the remaining classes of patterns for 8-PAM is left for further investigation as well as generalizing the results to arbitrary $M$. An extension of the
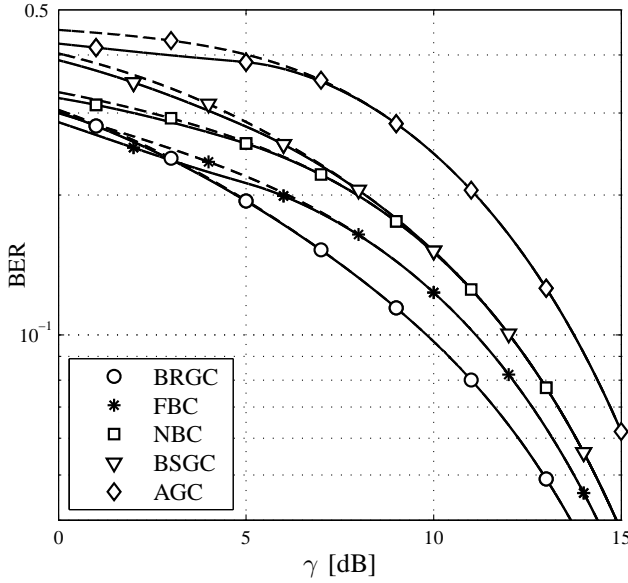
Fig. 5. The BER for 8-PAM with the 5 labelings in Table II. Solid lines correspond to the BD and dashed lines to the ABD.

present system model to other channel models is also left for future work.

## APPENDIX A
## PROOF OF THEOREM 4

Define the function $h(z)$ as

$$h(z) = \check{p}_4 A z^3 + \check{p}_3 z^2 + \check{p}_2 z + \check{p}_1 A. \quad (33)$$

According to Theorem 3, for 4-PAM with a pattern $\boldsymbol{p} = [p_1, p_2, p_3, p_4]$, equation $h(z) = 0$ needs to be solved in order to find the thresholds. The patterns for 4-PAM are either RE ($\check{p}_i = \check{p}_{M+1-i}, \forall i$) or ARE ($\check{p}_i = -\check{p}_{M+1-i}, \forall i$). Therefore

$$h(z) = \check{p}_1 A z^3 + \check{p}_2 z^2 \pm \check{p}_2 z \pm \check{p}_1 A, \quad (34)$$

where the upper and the lower signs correspond to RE and ARE patterns, resp. Using $\check{p}_i^2 = 1$ and the fact that $\check{p}_1 \check{p}_4 = \pm 1$ for RE and ARE patterns, resp., $h(z)$ can be factorized as

$$h(z) = \check{p}_1(z + \check{p}_1 \check{p}_4)(A z^2 + (\check{p}_1 \check{p}_2 - A \check{p}_1 \check{p}_4) z + A). \quad (35)$$

Solving $h(z) = 0$ gives the three roots $z_1 = -\check{p}_1 \check{p}_4$ and

$$z_{2,3} = \frac{\check{p}_1 \check{p}_4 A - \check{p}_1 \check{p}_2 \pm \sqrt{(\check{p}_1 \check{p}_4 A - \check{p}_1 \check{p}_2)^2 - 4A^2}}{2A}. \quad (36)$$

For $q = 1$ (where $\check{p}_1 \check{p}_4 = -1$ and $\check{p}_1 \check{p}_2 = 1$) the root $z_1 = 1$, that used in (16) gives the threshold $\beta_2 = 0$. The other two roots in (36) are complex for all SNR and do not result in thresholds.

In a similar way, for $q = 3$ (where $\check{p}_1 \check{p}_2 = -1$ and $\check{p}_1 \check{p}_4 = -1$) $\beta_2 = 0$. When $A \leq 1/3$, or equivalently, when $\gamma \geq 5 \log 3/8 \approx -1.63$ dB, the roots in (36) are real and positive resulting in thresholds $\beta_1$ and $\beta_3$ by using (16). When $A > 1/3$ (low SNR), the roots in (36) are complex and can no longer be used in (16) for calculating the thresholds. To overcome this, $|z_2|$ and $|z_3|$ are used in the calculation of the

thresholds, which together with $\check{p}_1 \check{p}_2 = -1$ gives (23). The use of $|\cdot|$ does not affect the result when the roots are real. When the roots are complex, their absolute values are equal to one (can be seen from (36)), which gives two virtual thresholds $\beta_1 = \beta_3 = 0$ merging with the zero-threshold $\beta_2$ at around $-1.63$ dB. Theorem 2 allows the use of these thresholds in the calculation of the PBER.

Finally, for $q = 2$ (where $\check{p}_1 \check{p}_2 = -1$ and $\check{p}_1 \check{p}_4 = 1$) $z_1 = -1$, which results in no threshold. The two roots in (36) are positive for all SNR, resulting in the thresholds $\beta_1$ and $\beta_3$ by using (16). As the roots are positive the use of $|\cdot|$ does not affect the result, which gives (23). This completes the proof.

## APPENDIX B
## PROOF OF THEOREM 5

Define the function $h(z)$ as

$$h(z) = \check{p}_8 A^6 z^7 + \check{p}_7 A^3 z^6 + \check{p}_6 A z^5 + \check{p}_5 z^4 + \check{p}_4 z^3 \\ + \check{p}_3 A z^2 + \check{p}_2 A^3 z + \check{p}_1 A^6. \quad (37)$$

According to Theorem 3 for 8-PAM with pattern $\boldsymbol{p} = [p_1, p_2, \ldots, p_8]$ equation $h(z) = 0$ needs to be solved in order to find the thresholds. For RE and ARE patterns, $\check{p}_i = \pm \check{p}_{M+1-i}, \forall i$, where the upper and the lower signs correspond to RE and ARE patterns, resp. Using this property, $h(z)$ for RE and ARE patterns is

$$h(z) = \check{p}_1 A^6 z^7 + \check{p}_2 A^3 z^6 + \check{p}_3 A z^5 + \check{p}_4 z^4 \\ \pm \check{p}_4 z^3 \pm \check{p}_3 A z^2 \pm \check{p}_2 A^3 z \pm \check{p}_1 A^6. \quad (38)$$

Factorizing (38) gives

$$h(z) = (z \pm 1)\left(\check{p}_1 A^6 z^6 + \left[\check{p}_2 A^3 \mp \check{p}_1 A^6\right] z^5 \\ + \left[\check{p}_1 A^6 \mp \check{p}_2 A^3 + \check{p}_3 A\right] z^4 + \left[\mp \check{p}_1 A^6 + \check{p}_2 A^3 \mp \check{p}_3 A + \check{p}_4\right] z^3 \\ + \left[\check{p}_1 A^6 \mp \check{p}_2 A^3 + \check{p}_3 A\right] z^2 + \left[\check{p}_2 A^3 \mp \check{p}_1 A^6\right] z + \check{p}_1 A^6\right). \quad (39)$$

Rearranging the terms in (39) $h(z)$ can be written as

$$h(z) = z^3(z \pm 1)\left(\check{p}_1 A^6(z^3 + z^{-3}) \\ + \left[\check{p}_2 A^3 \mp \check{p}_1 A^6\right](z^2 + z^{-2}) \\ + \left[\check{p}_1 A^6 \mp \check{p}_2 A^3 + \check{p}_3 A\right](z^1 + z^{-1}) \\ + \left[\mp \check{p}_1 A^6 + \check{p}_2 A^3 \mp \check{p}_3 A + \check{p}_4\right]\right). \quad (40)$$

Using the substitution

$$t(z) = z + z^{-1}, \quad (41)$$

and the relations

$$t(z^3) = t^3(z) + 3t(z), \quad (42)$$
$$t(z^2) = t^2(z) + 2, \quad (43)$$

(40) can be expressed as

$$h(z) = z^3(z \pm 1)\left(\check{p}_1 A^6 t^3(z) + \left[\check{p}_2 A^3 \mp \check{p}_1 A^6\right] t^2(z) \\ + \left[-2\check{p}_1 A^6 \mp \check{p}_2 A^3 + \check{p}_3 A\right] t(z) \\ + \left[\pm \check{p}_1 A^6 - \check{p}_2 A^3 \mp \check{p}_3 A + \check{p}_4\right]\right). \quad (44)$$

Finding positive roots of $h(z) = 0$ can now be done analytically. For ARE patterns the second factor in (44) gives

a root equal to one resulting in $\beta_4 = 0$. The roots of the last factor in (44) need to be found. As a first step we solve it with respect to $t(z)$, where the roots $t_n$ are shown in (26)–(28), where $\pm 1$ was replaced by $+\check{p}_1\check{p}_8$ to distinguish between RE and ARE patterns. As $z$ should be real and positive, only real and positive $t_n$ need to be considered. Two out of three roots $t_n$ may combine into a complex conjugated couple, but the third root is always real. Every positive root $t_n$ gives two roots for $z$ in (39), which can be found from (41) as

$$z_{2n-1,2n} = \frac{t_n \pm \sqrt{t_n{}^2 - 4}}{2}, \tag{45}$$

where $z_{2n-1} = 1/z_{2n}$. Due to (16) and the symmetry of the patterns, these two roots give the two thresholds $\beta_k = -\beta_{8-k}$, which justifies the first equality in (24). When $t_n$ is real and $t_n \geq 2$, the roots in (45) are positive and give thresholds $\beta_k = -\beta_{8-k}$. Because of $t_n$ is real and the roots $z_{2n-1}$ and $z_{2n}$ are positive, the use of $|\cdot|$ (three times) in (25) does not change the result. By analyzing all the roots $t_n$, the thresholds were found and listed in Table III, where the last column shows the relation between the threshold $\beta_k$ and the roots $t_n$ shown in (26)–(28).

For the listed thresholds in Table III, $t_n$ in (26)–(28) is never real and negative, however $t_n$ can be either complex or real with $0 \leq t_n < 2$ for some $\gamma < \gamma_0$, resulting in virtual thresholds $\beta_k$ and $\beta_{8-k}$. In what follows, we show that these thresholds are equal to each other when using (25), i.e., they fulfill the conditions in Theorem 2. First, consider the case when $t_n$ is real but $0 \leq t_n < 2$. In this case $z_{2n-1}$ and $z_{2n}$ are complex with unit magnitude and according to (24), the corresponding thresholds $\beta_k = -\beta_{8-k}$ are equal to zero. By analyzing the thresholds for all the RE and ARE patterns, we find that $\beta_5 = -\beta_3$ for $q = 3, 6, 9, 11$ and $\beta_6 = -\beta_2$ for $q = 5$, which are separated by either no threshold or by the threshold $\beta_4 = 0$. These thresholds can be used in (9) according to Theorem 2.

Second, consider the case when $t_n$ is complex. One of the other two roots of (44) $t_{n'}$ giving $\beta_{k'} = -\beta_{8-k'}$ is such that $t_{n'} = t_n{}^*$, which means that $|t_n| = |t_{n'}|$. This leads to two pairs of the thresholds $\beta_k = \beta_{k'}$ and $\beta_{8-k} = \beta_{8-k'}$. Revising the thresholds for all the RE and ARE patterns we conclude that corresponding thresholds are: $\beta_6 = -\beta_2$ and $\beta_7 = -\beta_1$ for $q = 8, 11$ and $\beta_5 = -\beta_3$ and $\beta_6 = -\beta_2$ for $q = 7, 10$. These thresholds can be used in (9) according to Theorem 2.

## References

[1] E. Zehavi, "8-PSK trellis codes for a Rayleigh channel," *IEEE Trans. Commun.*, vol. 40, no. 3, pp. 927–946, May 1992.

[2] G. Caire, G. Taricco, and E. Biglieri, "Bit-interleaved coded modulation," *IEEE Trans. Inf. Theory*, vol. 44, no. 3, pp. 927–946, May 1998.

[3] A. Guillén i Fàbregas, A. Martinez, and G. Caire, "Bit-interleaved coded modulation," *Foundations and Trends in Communications and Information Theory*, vol. 5, no. 1–2, pp. 1–153, 2008.

[4] M. K. Simon and R. Annavajjala, "On the optimality of bit detection of certain digital modulations," *IEEE Trans. Commun.*, vol. 53, no. 2, pp. 299–307, Feb. 1988.

[5] F. Gray, "Pulse code communications," U. S. Patent 2 632 058, Mar. 1953.

[6] E. Agrell, J. Lassing, E. G. Ström, and T. Ottosson, "On the optimality of the binary reflected Gray code," *IEEE Trans. Inf. Theory*, vol. 50, no. 12, pp. 3170–3182, Dec. 2004.

[7] E. Agrell, J. Lassing, E. G. Ström, and T. Ottosson, "Gray coding for multilevel constellations in Gaussian noise," *IEEE Trans. Inf. Theory*, vol. 53, no. 1, pp. 224–235, Jan. 2007.

[8] A. J. Viterbi, "An intuitive justification and a simplified implementation of the MAP decoder for convolutional codes," *IEEE J. Sel. Areas Commun.*, vol. 16, no. 2, pp. 260–264, Feb. 1998.

[9] Ericsson, Motorola, and Nokia, "Link evaluation methods for high speed downlink packet access (HSDPA)," TSG-RAN Working Group 1 Meeting #15, TSGR1#15(00)1093, Tech. Rep., Aug. 2000.

[10] P. Fertl, J. Jaldén, and G. Matz, "Performance assessment of MIMO-BICM demodulators based on mutual information," *IEEE Trans. Sig. Proc.*, vol. 60, no. 3, pp. 1366–1382, Mar. 2012.

[11] J. G. Proakis, *Digital Communications*, 4th ed. McGraw-Hill, 2000.

[12] M. K. Simon, S. M. Hinedi, and W. C. Lindsey, *Digital Communication Techniques: Signal Design and Detection*. Prentice Hall, 1995.

[13] K. Cho and D. Yoon, "On the general BER expression of one- and two-dimensional amplitude modulations," *IEEE Trans. Commun.*, vol. 50, no. 7, pp. 1074–1080, July 2002.

[14] P. J. Lee, "Computation of the bit error rate of coherent $M$-ary PSK with Gray code bit mapping," *IEEE Trans. Commun.*, vol. COM-34, no. 5, pp. 488–491, May 1986.

[15] J. Lassing, E. G. Ström, E. Agrell, and T. Ottosson, "Computation of the exact bit-error rate of coherent $M$-ary PSK with Gray code bit mapping," *IEEE Trans. Commun.*, vol. 51, no. 11, pp. 1758–1760, Nov. 2003.

[16] J. Lassing, E. G. Ström, E. Agrell, and T. Ottosson, "Unequal bit-error protection in coherent $M$-ary PSK," in *IEEE Vehicular Technology Conference (VTC-Fall)*, Orlando, FL, Oct. 2004.

[17] L. Szczecinski, C. Gonzalez, and S. Aissa, "Exact expression for the BER of rectangular QAM with arbitrary constellation mapping," *IEEE Trans. Commun.*, vol. 54, no. 3, pp. 389–392, Mar. 2006.

[18] J. Li, X. Zhang, Q. Gao, Y. Luo, and D. Gu, "Exact BEP analysis for coherent $m$-ary PAM and QAM over AWGN and Rayleigh fading channel," in *IEEE Vehicular Technology Conference (VTC-Spring)*, Singapore, May 2008.

[19] M. Ivanov, F. Brännström, A. Alvarado, and E. Agrell, "General BER expression for one-dimensional constellations," in *IEEE Global Communications Conference (GLOBECOM)*, Anaheim, CA, Dec. 2012.

[20] E. Agrell and A. Alvarado, "Optimal alphabets and binary labelings for BICM at low SNR," *IEEE Trans. Inf. Theory*, vol. 57, no. 10, pp. 6650–6672, Oct. 2011.

[21] S. ten Brink, J. Speidel, and R.-H. Yan, "Iterative demapping and decoding for multilevel modulation," in *IEEE Global Telecommunications Conference (GLOBECOM)*, Sydney, Australia, Nov. 1998.

[22] P. Robertson, E. Villebrun, and P. Hoeher, "A comparison of optimal and sub-optimal MAP decoding algorithms operating in the log domain," in *IEEE International Conference on Communications (ICC)*, June 1995.

[23] K. Hyun and D. Yoon, "Bit metric generation for Gray coded QAM signals," *IEEE Proc.-Commun.*, vol. 152, no. 6, pp. 1134–1138, Dec. 2005.

[24] M. S. Raju, R. Annavajjala, and A. Chockalingam, "BER analysis of QAM on fading channels with transmit diversity," *IEEE Trans. Wireless Commun.*, vol. 5, no. 3, pp. 481–486, Mar. 2006.

[25] E. Akay and E. Ayanoglu, "Low complexity decoding of bit-interleaved coded modulation for $M$-ary QAM," in *IEEE International Conference on Commununications (ICC)*, Paris, France, Jun. 2004.

[26] R. Ghaffar and R. Knopp, "Low complexity metrics for BICM SISO and MIMO," in *IEEE Vehicular Technology Conference (VTC-Spring)*, Taipei, Taiwan, May 2010.

[27] M. Benjillali, L. Szczecinski, S. Aissa, and C. Gonzalez, "Evaluation of bit error rate for packet combining with constellation rearrangement," *Wiley Journal Wireless Comm. and Mob. Comput.*, pp. 831–844, Sep. 2008.